THE PETROGENETIC HISTORIES OF LUNAR MAGMATIC SYSTEMS AS TOLD BY APOLLO BASALT CRYSTAL CARGOES. A. J. Gawronska[1], C. L. McLeod[1], M. Loocke[2], B. Shaulis[3], [1]Department of Geology and Environmental Earth Science, Miami University, Oxford OH (gawronaj@miamioh.edu). [2]Chevron Geomaterials Characterization Laboratory, Department of Geology and Geophysics, Louisiana State University, Baton Rouge LA. [3]Trace Element and Radiogenic Isotope Laboratory, University of Arkansas, Fayetteville AR.

Introduction: Extruded igneous rocks preserve evidence of the physical processes associated with their petrogenesis. By studying the crystal stratigraphy of mineral grains such processes (e.g., magma mixing or convection during storage, transport, and/or eruption) can be evaluated [1-2]. For example, combined textural and chemical analysis from core to rim can reveal changes in the magmatic environment during crystal growth, both prior to and during eruption [1-2].

On Earth, crystal-scale approaches to investigating magmatic systems have led researchers to identify distinct crystal populations with unique petrogenetic histories preserved in the same igneous rock [e.g., 3]. Following recent summary of petrologic terminology by Zellmer [4], crystals formed in the magma batch that transported the crystal cargo to the surface can be preserved as autocrysts; crystals formed in a separate but petrogenetically related magma batch are antecrysts; crystals that are not petrogenetically related to the carrier magma are xenocrysts [3]. Collectively, such crystal populations form the "crystal cargo" of a rock, but each preserve their own individual petrogenetic story. Here, an investigation of the crystal stratigraphy [e.g., 2-3, 5] of major silicate minerals (pyroxene, plagioclase feldspar, olivine) was employed to study the petrogeneses of six Apollo basalts. In order to evaluate how similarly/differently magmatic processes may have operated on a Moon-wide scale (within the constraints of the landing sites chosen during the Apollo program), samples from different missions and with different chemical and textural characteristics were chosen.

Sample descriptions: Samples chosen include: 1) high-K, high-Ti fine-grained Apollo 11 sample 10057, 2) low-Ti feldspathic and medium-grained Apollo 12 sample 12038; 3) low-Ti and porphyritic Apollo 12 sample 12043; 4) low-Ti and microgabbroic Apollo 15 sample 15085; 5) low-Ti, highly vesiculated Apollo 15 sample 15556; and 6) the high-Ti, coarse-grained Apollo 17 sample 70017.

Methods: Initial petrographic characterization of sample thin sections was completed on a Leica polarized light microscope in-house at Miami University. This was followed by major element mapping of whole thin sections on a Zeiss Supra 35 VP FEG scanning electron microscope at the Center for Advanced Microscopy and Imaging at Miami University. Together these datasets were used to generate crystal size distribution plots (CSD) for plagioclase and ilmenite in each of the samples, following the methods outlined in [6].

Next, concentrations of major elements in silicate phases were quantified in-situ via electron probe microanalysis. This was accomplished on a JEOL JXA-8230 electron microprobe at Louisiana State University. Subsequently, in-situ analysis of trace elements in silicate phases is planned via laser ablation inductively coupled plasma mass spectrometry on a NWR193 laser ablation system connected to a Thermo Icap Q ICP-MS at the University of Arkansas.

Results and Discussion: CSD analyses [see 6] of plagioclase and ilmenite indicate that samples 12043, 15556, and 70017 experienced an abrupt change in their growth environment. Moreover, sample 70017 may preserve evidence of plagioclase and pyroxene coarsening. In all samples, plagioclase grains are generally subhedral to euhedral. Plagioclase is not

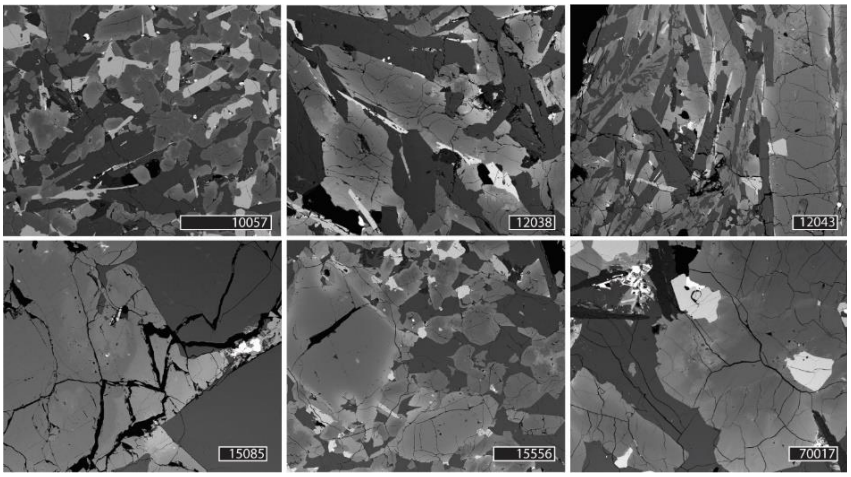

Figure 1: Backscatter electron images of representative textures in each of the samples investigated here. Scale bar is 250 microns in all images.

significantly zoned with respect to major elements (see figs. 2-3), which indicates that plagioclase crystallized under conditions close to equilibrium in all samples.

Notably, pyroxene in all samples is zoned (see figs. 4-5). Most pyroxene grains are normally zoned, while some grains contain abrupt and irregular contacts between different growth zones, which is interpreted here as preserving evidence of reaction between crystal and melt and subsequent resorption before further growth (see 15085 in fig. 1). Abrupt zoning in such cases is accompanied by a change in composition, potentially indicating an abrupt change in the melt environment surrounding the grain during growth. Such zones generally correspond to an increase in Mg and Ca content (fig. 3) and correspond to disequilibrium textures identified via light microscopy. Moreover, samples 15085, 15556, and 70017 contain symplectites where high-Fe pyroxene is breaking down to form fayalite, silica, and lower-Fe pyroxene. This breakdown over time may be due to phase instability or shock metamorphism during impact [8].

Complementary in-situ trace element analysis will soon supplement the work described here. Altogether, this project will shed light on the magmatic processes which operated during the evolution of lunar magmatic systems and will reveal the extent to which these processes were open or closed in their nature. This has implications for the petrogenetic interpretations attributed to the entire lunar igneous rock suite, especially where autocrystic or antecrystic crystal cargoes are found [3-4], which have been documented to affect whole rock compositions [e.g., 9].

Acknowledgments: This work was funded through GSA Graduate Student Research Grant #13203-21 to author Aleksandra Gawronska.

References: [1] Edmonds et al. (2019) Phil. Trans. R. Soc. A 377:20180298. [2] Ubide et al. (2019) Front. Earth Sci. 7:239. [3] Davidson et al. (2007) Annu. Rev. Earth Planet Sci. 35:273. [4] Zellmer, G. (2021) Bull. Volcanol. 83:77. [5] Hui et al. (2011) Geochim. et Cosmochim. Acta 75(21):6439. [6] Higgins (2000) Am. Min. 85:1105. [7] Miao et al. (2013) Met. Soc. #5234. [8] Ubide et al. (2014) Lithos 206-207:214.

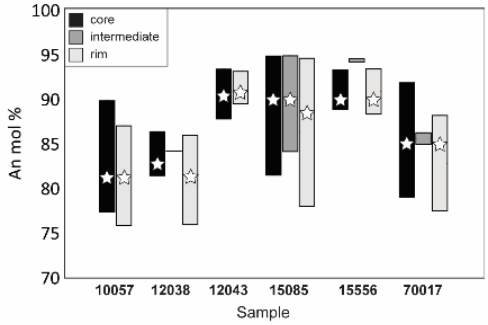

Figure 2: Change in plagioclase anorthite content from core to rim. Star represents the average composition.

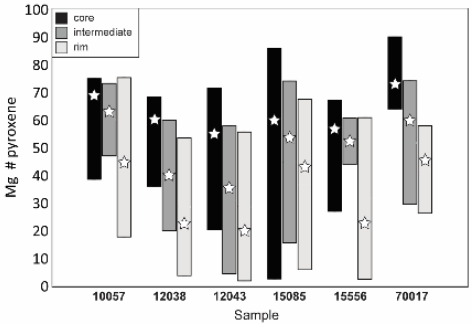

Figure 4: Change in pyroxene Mg# from core to rim. Star represents the average composition.

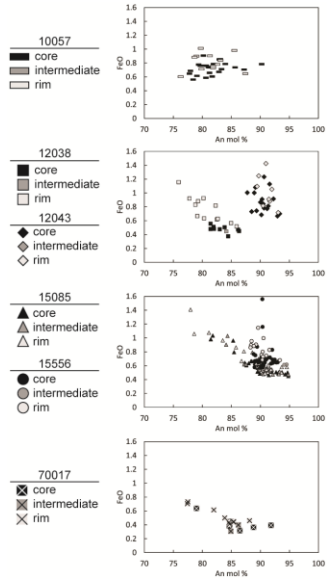

Figure 3: Core to rim change in plagioclase composition.

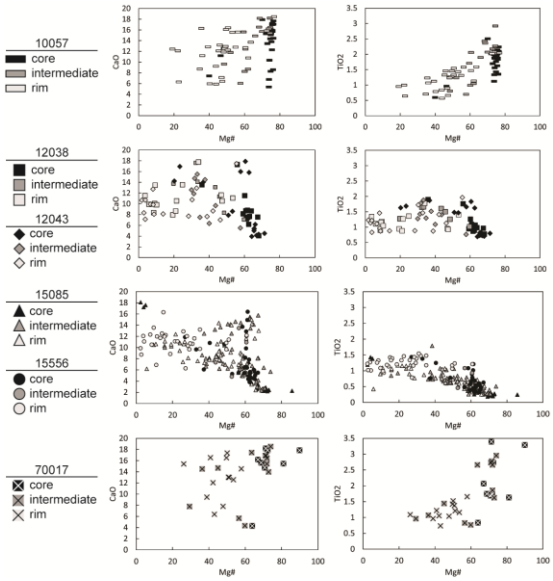

Figure 5: Core to rim change in pyroxene composition.